

# AerialVG: A Challenging Benchmark for Aerial Visual Grounding by Exploring Positional Relations

Junli Liu<sup>\*1,2</sup> Qizhi Chen<sup>\*2,3</sup> Zhigang Wang<sup>\*2</sup> Yiwen Tang<sup>1</sup> Yiting Zhang<sup>2,3</sup>  
 Chi Yan<sup>2</sup> Dong Wang<sup>2</sup> Xuelong Li<sup>4</sup> Bin Zhao<sup>1,2</sup>

<sup>1</sup>Northwestern Polytechnical University <sup>2</sup>Shanghai AI Laboratory <sup>3</sup>Zhejiang University <sup>4</sup>TeleAI



Figure 1. **Overview of AerialVG.** This work introduces aerial visual grounding (AerialVG), a new task for intelligent drones. We provide the first dataset for this task, consisting of 50K annotations and 103K objects. Additionally, an AerialVG model is proposed to explore the positional relations among objects and achieve superior context-aware visual grounding in drone applications.

## Abstract

Visual grounding (VG) aims to localize target objects in an image based on natural language descriptions. In this paper, we propose AerialVG, a new task focusing on visual grounding from aerial views. Compared to traditional VG, AerialVG poses new challenges, e.g., appearance-based grounding is insufficient to distinguish among multiple visually similar objects, and positional relations should be emphasized. Besides, existing VG models struggle when applied to aerial imagery, where high-resolution images cause significant difficulties. To address these challenges, we introduce the first AerialVG dataset, consisting of 5K real-world aerial images, 50K manually annotated descrip-

tions, and 103K objects. Particularly, each annotation in AerialVG dataset contains multiple target objects annotated with relative spatial relations, requiring models to perform comprehensive spatial reasoning. Furthermore, we propose an innovative model especially for the AerialVG task, where a Hierarchical Cross-Attention is devised to focus on target regions, and a Relation-Aware Grounding module is designed to infer positional relations. Experimental results validate the effectiveness of our dataset and method, highlighting the importance of spatial reasoning in aerial visual grounding. The code will be released at <https://github.com/Ideal-ljl/UAVVG>.

## 1. Introduction

Visual Grounding (VG) is a challenging task that involves identifying specific regions or objects within an image following natural language instructions. This task requires models to deeply understand both visual and textual modalities, effectively aligning image context with corresponding linguistic expressions. VG is critical for a wide range of applications, including visual question answering, vision-and-language navigation, and human-robot interaction, *etc* [22, 45, 52].

With the continuous progress of multimodal models, the performance of VG tasks has been significantly improved. However, existing models and datasets still have obvious limitations. Current research focuses primarily on ground-based object, and the exploration of aerial visual grounding remains underdeveloped. Aerial visual grounding has significant potential applications in areas such as emergency rescue, logistics, and ecological monitoring, which calls for further research and development. Specifically, the ability to manage multiple objects of the same type and their spatial relationships in complex environments remains underdeveloped, leading to limited generalization capabilities in real-world scenarios.

To this end, we propose a more challenging task, termed Aerial Visual Grounding (AerialVG). AerialVG aims to apply the visual grounding task to UAV platforms, and promote the development of UAV intelligent perception and autonomous navigation technologies. Compared with traditional VG tasks, AerialVG faces more challenges, mainly in the following two aspects:

- **Broad field of view and small objects.** Unlike images from the ground perspective, when UAVs capture images from the air, the field of view is usually much broader, and the size of objects in the image tends to be relatively small. While a larger field of view provides more context and coverage, it also imposes challenges to locate and identify objects at a finer scale.
- **Complex object distribution and spatial relationship.** From the perspective of UAVs, object types are mainly pedestrians and vehicles, which are usually distributed in crowded urban environments. Especially in busy urban streets or traffic-intensive areas, there may be multiple similar or identical objects in the field of view at the same time. For example, multiple similar vehicles are often simultaneously presented in one street. In this case, it is difficult to accurately distinguish the target object based on appearance features alone, and it is necessary to rely on the spatial relationship between objects, such as relative position, distance, and direction, to achieve precise positioning and recognition.

To address above issues, we propose the first dataset designed specifically for the AerialVG task. The dataset consists of 5,000 high-resolution images covering a variety of

complex urban environments and contains a rich variety of object types, such as pedestrians, vehicles, and other common urban objects. In addition, the dataset includes nearly 50k manual annotations. These annotations not only provide the bounding box of each object but also include natural language descriptions related to the object, which can help the model understand the positional relationship between objects. With these high-quality annotations, a comprehensive and efficient test platform is provided for the AerialVG task.

Aiming at the core challenges in the AerialVG task, we also design an innovative model that can accurately locate objects based on the positional relation between them. Specifically, a Hierarchical Cross-Attention is first proposed to help the model focus more effectively on regions where objects are most likely to appear, thus addressing the issue of vast visual areas. Furthermore, we devise a Relation-Aware Grounding module to understand spatial information such as the relative position, direction, and distance between objects, effectively distinguishing multiple similar objects.

Overall, the main contributions of this work are summarized as follows:

- We propose the AerialVG task and introduce the first dataset, providing a valuable resource for advancing research in aerial visual grounding.
- We present a novel AerialVG model that effectively addresses two key challenges, *i.e.*, the large field of view with small-sized objects and the complex distribution and spatial relationships between objects.
- We conduct extensive experiments to thoroughly validate the effectiveness of our proposed model, demonstrating its superior performance.

## 2. Related Work

**Visual Grounding.** Visual Grounding (VG) is a fundamental task that requires identifying specific objects in an image based on natural language descriptions. This task has made some progress in both 2D [5, 25] and 3D [17, 18, 36–38, 47, 50] fields. Existing visual grounding methods can be broadly divided into two categories, *i.e.*, (1) two-stage methods[13, 28, 41] and (2) one-stage methods[27, 34, 35]. The former first generates region-level candidate boxes and then uses language to select the best matching region. The latter directly interacts with visual and language cues through bounding boxes, avoiding the computationally intensive proposal box generation and region feature extraction steps present in two-stage methods. Several recent methods[8, 10, 23, 25] have adopted the transformer structure for multimodal fusion, thus achieving better performance. In addition, with the booming development of vision language models (VLMs), some studies [42, 43, 48] have improved the performance of vision grounding by fine-

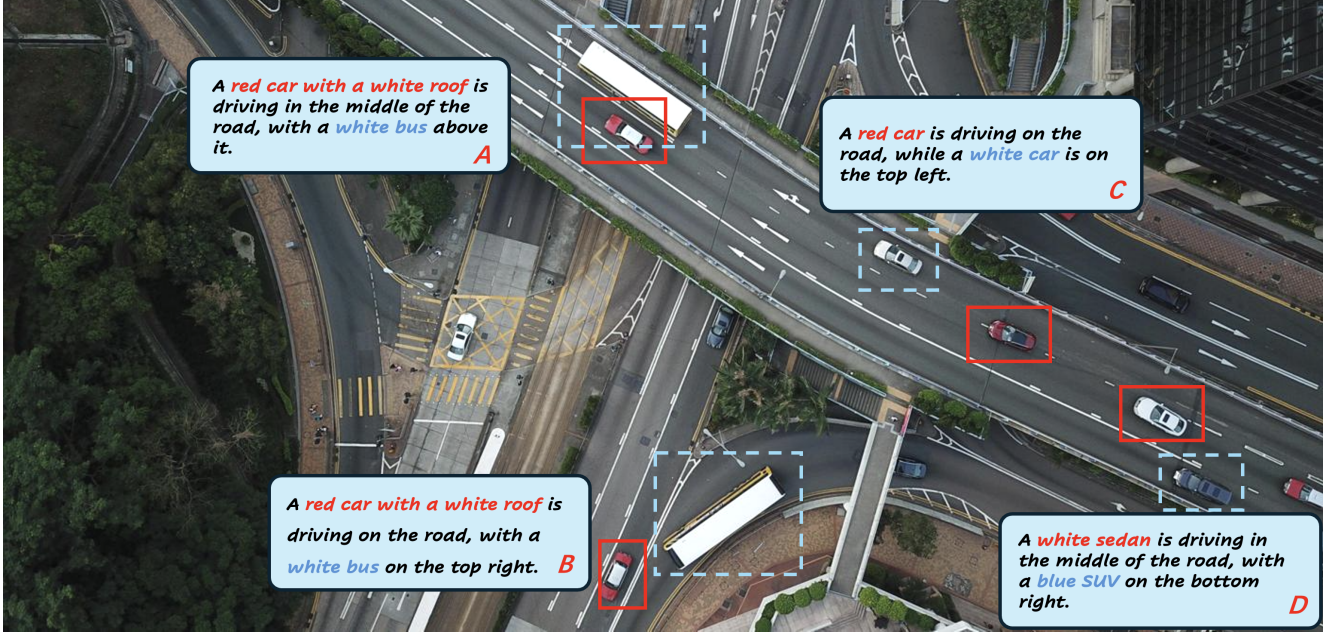


**Figure 2. Example of AerialVG Dataset.** There are many red cars in the picture. In order to achieve accurate object positioning, we need to use the positional relationship of surrounding auxiliary objects to assist reasoning. To this end, we accurately annotated the data to ensure that the spatial relationship between objects can be fully captured, thereby improving the accuracy of AerialVG.

tuning pre-trained VLMs, making full use of the knowledge and advantages of pre-trained models. These advances have improved both the accuracy and efficiency of VG systems, enabling more complex applications. However, they still cannot solve the spatial relationship problem in AerialVG.

**Vision-Language Models.** Vision-Language Models (VLMs) integrate visual and linguistic information to perform tasks that require both image understanding and natural language processing. Typically, they use pretrained visual backbones to encode images, and large-scale language models to interpret textual inputs. The visual and textual information is then fused through mechanisms like cross-attention layers. Recent advancements, such as GPT-4o [31], LLaVA [24], and InstructBLIP [6], have achieved significant progress in language-guided navigation and visual reasoning. VLMs have also been adapted to a variety of domains. Specifically, robot action generation produces robot actions based on textual instructions [33, 51], vision language navigation guides UAVs in aerial environments [14, 26], 3D generation creates and understands 3D data based on language inputs [39, 44]. Moreover, VLMs are increasingly used in video understanding, biomedical imaging, and remote sensing, demonstrating their versatility across different tasks. These developments highlight the growing potential of VLMs in various real-world applications.

**Spatial Reasoning Representation.** Spatial reasoning, traditionally part of broader tasks like SLAM [1, 11] or

depth estimation [12], has seen increasing interest in the context of VLMs. Earlier research focused on explicit spatial scene representations, such as spatial memory [15, 16] or spatial scene graphs [19, 40], to help machines understand and reason about spatial relations. Recent work has further advanced the spatial reasoning capabilities of VLMs. Some approaches leverage 3D information to enhance VLM performance. [3, 20, 21, 32] focus on reconstructing scenes from multi-view images and integrating dense semantic features to improve these representations. These 3D representations are then fused into LLMs for better spatial understanding. However, multi-view images are not always available, and the explicit construction of scenes using dense semantic features can be computationally intensive. Furthermore, the gap between 3D representations and language can often degrade performance. In contrast, other approaches utilize 2D VLMs to understand spatial relationships and measure distances. Unlike the 3D methods, spatial understanding in these models is implicitly encoded, allowing the VLM to directly address spatial reasoning tasks without requiring explicit 3D representations or scene graphs, as seen in works like [2, 4].

### 3. Dataset

In this paper, we develop the AerialVG dataset as shown in Figure 2. This dataset contains 5,000 high-definition images taken from UAVs. We annotated them to ensure that they are suitable for aerial visual grounding task. In addition, we

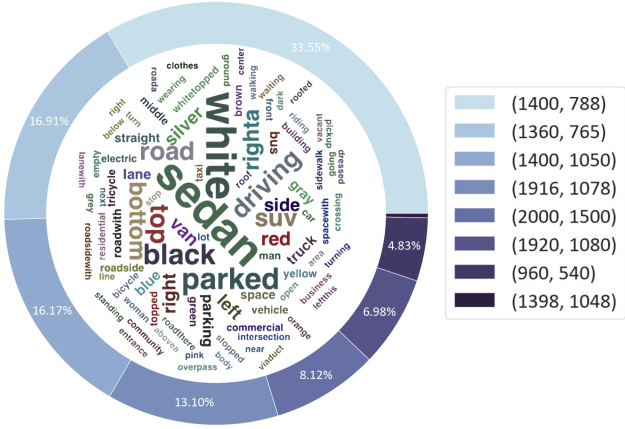


**Figure 3. Resolution distribution and word cloud of AerialVG dataset.** Most of the images in AerialVG dataset are high-resolution, and the most frequently appearing words are vehicle type, color, and location.

provide a specially designed natural language description for each object, which details the objects in the image and their relative positions. The AerialVG dataset provides a solid foundation for fine-grained object grounding in complex scenes from a high-altitude perspective, and especially lays a new research direction for the efficient grounding and understanding tasks of intelligent UAVs.

### 3.1. Dataset generation

The images in our AerialVG dataset are sourced from the VisDrone2019 dataset [53]. VisDrone consists of 288 video clips (261,908 frames) and 10,209 static images captured by various UAV-mounted cameras across 14 cities, covering a range of environments such as urban and rural areas. This diversity in scene type, location, and conditions (including different weather and lighting) offers a robust foundation for visual grounding tasks. The dataset includes more than 2.6 million manually annotated bounding boxes, highlighting common objects like pedestrians, vehicles, and bicycles, with attributes such as visibility, object class, and occlusion.

In UAV-view images, buildings and roads occupy most of the visual space, while the primary objects of interest are pedestrians and vehicles. They often exhibit similar appearances. Relying solely on coarse-grained categories is insufficient for accurate object localization. Therefore, the annotations must capture fine-grained object features, *e.g.*, color, vehicle type, clothing, and consider the spatial relationships between target objects and prominent surrounding elements. Due to the complexity of visual annotation, we opted for manual annotation to ensure precision.

Our manual annotation process follows these principles:

- **Observer-perspective spatial relationships.** For the convenience of annotation and unification, our position relation is described from the first-person perspective and

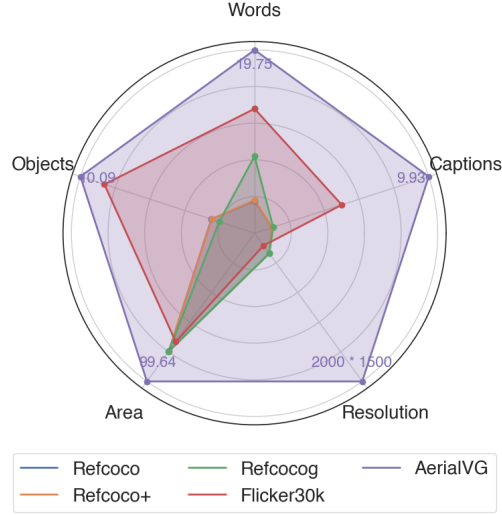


**Figure 4. Comparison between different datasets.** Words refers to the average number of words in the text; Objects refer to the average number of objects in each image; Area refers to the proportion of irrelevant areas; Resolution refers to the maximum resolution of the dataset images and Captions refers to the average number of annotations contained in each image.

is divided into eight categories, *i.e.*, above, below, left, right, top left, top right, bottom left, and bottom right. As shown in Figure 2 A, the white bus is above the red car with a white roof, not on the right.

- **Selection of prominent auxiliary objects.** When locating the target object, we give priority to selecting the closest object as the auxiliary object to improve positioning accuracy. To ensure simplicity, if one auxiliary object is sufficient to locate the target, no redundant description will be provided. For instance, as shown in Figure 2 D, the target object is the white sedan, and we select the blue SUV as the auxiliary object, while disregarding the red car at the top left.

### 3.2. Dataset statistics

This subsection presents key statistics of the AerialVG dataset and offers a comparative comparison with existing visual grounding datasets.

Figure 3 shows the resolution distribution and word cloud for the AerialVG dataset. Unlike the RefCOCO series, where over 70% of images have a resolution around  $600 \times 650$ , the AerialVG dataset consists mostly of images with resolutions greater than  $1000 \times 500$ . This higher resolution and wider field of view make the Aerial VG task more challenging.

The word cloud analysis highlights frequent mentions of vehicle types, colors, and spatial positions. These annotations emphasize the importance of understanding not only object identification but also their relative locations in the environment. This rich annotation style is critical for tasks

like UAV navigation, emergency response, and large-scale monitoring, where spatial relationships are essential for accurate decision-making.

Figure 4 compares the AerialVG dataset with existing visual grounding datasets across three key aspects, *i.e.*, the average number of words in the text, the average number of objects located in the image, and the proportion of irrelevant regions. In all three aspects, the AerialVG dataset demonstrates a higher level of challenge, highlighting its complexity and suitability for more advanced visual grounding tasks.

## 4. Method

As shown in Figure 5, we take GroundingDINO [25] as the baseline and design an end-to-end model for AerialVG. GroundingDINO [25] is built on a transformer architecture, where the encoder stacks self-attention and cross-attention layers to fuse image and text features. After fusing these multimodal features, it selects the most relevant features as queries, which are highly similar to the text. These queries are then decoded in the decoder, and the final bounding boxes and logits are generated by the bbox head and class head, respectively.

Unlike GroundingDINO [25], after embedding the image into hierarchical features using Swin-Transformer [29], we fuse these features with text features encoded by BERT [9] via Hierarchical Cross Attention, enabling the model to focus more on potential regions where objects are likely to appear. After the Decoder, we introduce the Relation-Aware Grounding module to capture the positional relationships between different objects.

### 4.1. Hierarchical Cross-Attention

In aerial view images, high resolution often comes with large portions of the scene occupied by buildings, roads, and other background elements, reducing the focus on key objects. To address this, we propose Hierarchical Cross-Attention, a mechanism designed to help the model more efficiently attend to relevant areas within the scene.

With the hierarchical feature representation enabled by Swin-Transformer[29], image features are organized in a layered manner. However, traditional cross-attention methods typically compute a complete attention map by flattening the features for processing, which can lead to information loss during the subsequent fusion process. In hierarchical structures, features at the same spatial location across different layers still represent the same object. Therefore, if a high-attention region is identified in one layer based on textual cues, this region should receive increased attention in subsequent layers. Conversely, if a region shows low attention, it can be partially disregarded in the next layer, enabling the model to prioritize more relevant areas effectively.

As shown in Figure 5, after calculating the attention map between textual and image features, we retain their hierarchical structure. As the layer number increases, the attention map will also become smaller, making small objects receive insufficient attention in the higher layers. To alleviate this problem, we first convolve the attention map of the first layer to make it consistent with the shape of the last layer map, and fuse the result with it.

$$A_n^* = (1 - \beta) \times A_n + \beta \times C(A_1), \quad (1)$$

where  $C(\cdot)$  denotes the convolution operation,  $\beta$  is a hyper-parameter,  $A_j$  represents the attention map of the  $j$ -th layer. The processed attention map is then combined with the highest layer’s attention map  $A_n$ , ensuring that even small objects are given adequate focus. After that, we use Equation 2 to enhance the attention map in lower layers based on the higher layers.

$$A_i^* = (1 - \alpha) \times A_i + \alpha \times F(A_{i+1}). \quad (2)$$

Specifically, we use bilinear interpolation  $F(\cdot)$ , to expand the attention map  $A_{i+1}$  of the  $i + 1$  layer to the shape of the  $i$  layer  $A_i$ . The expanded attention map is then weighted by the hyper-parameter  $\alpha$  and combined with  $A_i$  to form the updated  $A_i^*$ . This approach effectively achieves our goal without introducing additional parameters, yielding improvements in performance.

### 4.2. Relation-Aware Grounding

Following GroundingDINO [25], we first perform language-guided query selection after the encoder, and then pass the selected queries into the decoder. In the decoder, we perform cross-attention on the query separately with the image features and text features to enhance the model’s ability to localize objects. However, experiments showed that these features did not adequately capture the positional relations described in the text.

We draw inspiration from certain 3D visual grounding methods for determining spatial relationships. However, those methods generally require explicit bounding boxes and clearly defined spatial relationships, rather than leveraging full textual descriptions. Our approach circumvents these requirements while still achieving competitive results.

Specifically, we design a Relation-Aware Grounding module to capture positional relation information. As shown in figure 5, after passing through the decoder, the fused features already contain the positional information of each object. Assuming we have  $m$  features before the Relation-Aware Grounding module, we then concatenate every two of the  $m$  features in pairs to obtain  $m^2$  features, which effectively captures the pairwise relationships between the objects and enhances the model’s ability to learn these interactions. The self-attention operation is performed

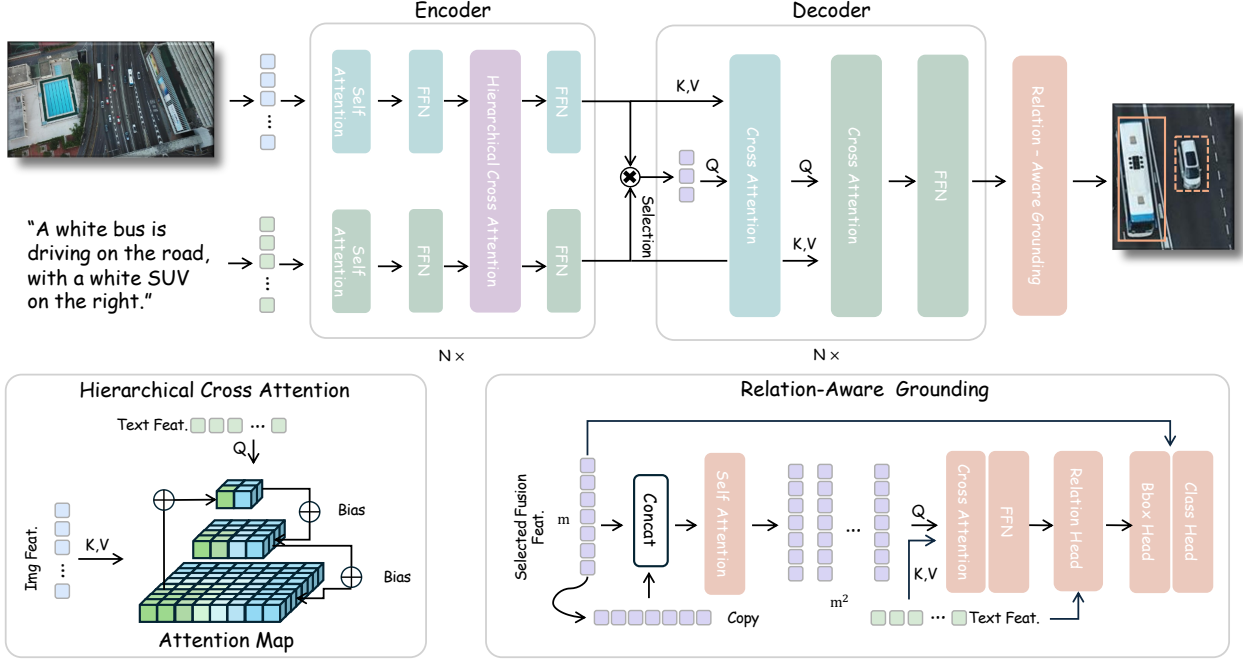


Figure 5. **The architecture of AerialVG model.** Hierarchical Cross Attention directs the model’s focus to potential object locations, while the Relation-Aware Grounding module enables the model to perceive spatial relationships between objects.

on  $m$  concatenated features in the same column to perceive the positional relation between objects. Subsequently, we conduct cross-attention with  $m^2$  queries and the text features. This step enables the model to better align and integrate both visual and textual information, enhancing its understanding of the contextual relationships between objects.

Finally, we first map the last state of the hidden layer to the specified feature dimension through the Relation Head. On this basis, we calculate the similarity between these features and the text features. The calculated similarity scores are then subjected to a softmax operation to generate a set of normalized similarity values. These normalized values represent the relationship score between each pair of objects, that is, how well they match the relationship described in the text. In this way, we can get an  $m \times m$  relationship matrix, which represents the relationship score between each pair of objects. We take the maximum value from each row of this relationship matrix as the final relation score for each object. We combine the relation scores with the scores obtained from the query through the class head to form the final logits.

#### 4.3. Loss Function

Our loss function consists of three parts, *i.e.*,  $\mathcal{L}_{\text{reg}}$ ,  $\mathcal{L}_{\text{cls}}$  and  $\mathcal{L}_{\text{rel}}$  as shown in Equation 3.

$$\mathcal{L} = \mathcal{L}_{\text{reg}} + \mathcal{L}_{\text{cls}} + \mathcal{L}_{\text{rel}}. \quad (3)$$

Following previous work on GroundingDINO, we employ L1 loss and GIOU loss for bounding box regression in  $\mathcal{L}_{\text{reg}}$ .

For classification, we adopt a contrastive loss between predicted objects and language tokens as  $\mathcal{L}_{\text{cls}}$ , in line with the GLIP [49] approach.

Additionally, we compute a Relation Loss based on the predicted relationships between object pairs.

$$\mathcal{L}_{\text{rel}} = -\log \left( \frac{e^{m_{i,j}}}{\sum_{i,j} e^{m_{i,j}}} \right), \quad (4)$$

where Hungarian matching is performed to identify the corresponding target object  $m_i$  and the auxiliary object  $m_j$ . In this way, the element  $m_{i,j}$  of the  $m \times m$  relationship matrix represents the ground truth relation between the objects. We then use Equation 4 to maximize the score at the corresponding position  $m_{i,j}$  in the relation matrix.

## 5. Experiment

### 5.1. Implementation Details

Our proposed AerialVG model, utilizes Swin-L [29] as the image backbone. For text representation, we employ the BERT-base [9] from Hugging Face as the text backbone. Following Grounding DINO, we extract four levels of image feature scales from the image backbone, ranging from  $4\times$  to  $32\times$ . We set the maximum number of text tokens to 256. We set  $N = 6$  for Encoder and Decoder layers, while the Relation-Aware Grounding module consists of three layers. The final loss function consists of multiple components, *i.e.*, classification loss (or contrastive loss), L1 loss, GIoU loss, and relation loss, with corresponding weights set

to 1.0, 5.0, 2.0, and 1.0, respectively. The hyper-parameters  $\alpha$  and  $\beta$  are set to 0.2 and 0.3. We conduct extensive experiments on the AerialVG dataset and the RefCOCO [46], RefCOCO+ [46], and RefCOCOg [30] datasets. Additionally, we perform ablation studies to demonstrate the effectiveness of our model design.

Our model training consists of two stages. Initially, we train the model without the Relation-aware Grounding module, using existing VG datasets following Grounding DINO [25] to achieve convergence. Once the model has converged, we freeze all other parameters and train the Relation-Aware Grounding module using our AerialVG dataset only, allowing it to specifically capture inter-object relationships. More details can be found in our supplementary material.

## 5.2. Evaluation metric

In AerialVG, object homogeneity is a significant challenge, as many objects share nearly identical visual characteristics. A model that performs well on Top-5 Accuracy but poorly on Top-1 Accuracy likely relies primarily on visual similarity rather than understanding the spatial relationships or contextual cues that distinguish between objects. By analyzing both Top-1 and Top-5 Accuracy, we can diagnose specific failure modes of the model. Model with both high Top-1 and Top-5 Accuracy demonstrates strong object discrimination and contextual understanding ability, making it more reliable for AerialVG-related applications.

Table 1. Performance comparison on the AerialVG dataset.

Method	Setting			
	Zero-Shot		Fine-Tuning	
	Top 1	Top 5	Top 1	Top 5
TranVG[8]	2.57	3.65	11.53	13.68
Dynamic-MDETR[7]	2.61	4.63	19.87	29.87
SimVG[5]	3.61	4.68	20.94	31.32
Grounding DINO[25]	11.10	13.79	29.36	78.87
AerialVG(Ours)	-	-	<b>50.01</b>	<b>87.00</b>

## 5.3. Results

Table 1 presents the evaluation results of different models on the AerialVG dataset. In the Zero-Shot setting, existing VG models exhibit limited performance, with both Top-1 Accuracy and Top-5 Accuracy hovering around 10%. This result highlights the challenges posed by high-resolution aerial imagery and the unique characteristics of the aerial viewpoint, which are not well-represented in existing datasets. The poor performance of these models further underscores the necessity of AerialVG as a benchmark for evaluating visual grounding in aerial scenes.

After fine-tuning, Top-5 Accuracy shows a significant improvement, indicating that models can better recognize and retrieve relevant object candidates when adapted to the AerialVG. However, Top-1 Accuracy remains relatively low, suggesting that while models are able to identify visually similar objects within the scene, they struggle to distinguish the correct target based on spatial relationships and contextual cues.

In comparison, the proposed AerialVG model demonstrates superior performance over previous approaches. It demonstrates a better understanding of object relationships in aerial images, resulting in higher Top-1 and Top-5 accuracy. This suggests that our model effectively integrates the Hierarchical Cross-Attention mechanisms and the Relation-Aware Grounding module, which are crucial for distinguishing visually similar objects based on spatial dependencies. These results validate our architectural choices and demonstrate the effectiveness of our model in addressing the unique challenges of aerial visual grounding.

In addition to the AerialVG dataset, we also evaluate our AerialVG model on the RefCOCO[46], RefCOCO+[46], and RefCOCOg[30] datasets to assess its performance on standard visual grounding benchmarks. As shown in Table 2, our AerialVG model also presents good performance across multiple metrics on the RefCOCO series datasets, achieving comparable results with previous state-of-the-art approaches.

These findings confirm that the integration of the Hierarchical Cross-Attention and Relation-Aware Grounding module does not compromise the model’s ability to accurately localize individual objects. Despite being designed to enhance spatial reasoning and relational understanding, these components maintain strong object-level grounding capabilities. This highlights the versatility of our model, making it effective in both aerial imagery and conventional ground-based VG tasks.

## 5.4. Ablation study

To further validate the effectiveness of the Hierarchical Cross-Attention and the Relation-Aware Grounding module, we conduct ablation experiments, as shown in Table 3. The results demonstrate that each component plays a crucial role in improving different aspects of the model’s performance.

- Hierarchical Cross-Attention significantly enhances Top-5 Accuracy, indicating that this module helps the model focus on fine-grained details within the image. By attending to multi-level image features, the model can better capture subtle differences between similar objects, leading to improved candidate retrieval.
- Relation-Aware Grounding module notably improves Top-1 Accuracy, demonstrating its ability to refine object selection by incorporating relational reasoning. This con-

Table 2. Performance comparison on RefCOCO, RefCOCO+, and RefCOCOg datasets.

Method	Backbone	RefCOCO			RefCOCO+			RefCOCOg	
		val	testA	testB	val	testA	testB	val	test
TranVG [8]	ResNet-101	80.32	82.67	78.12	63.5	68.18	55.63	67.11	67.44
Dynamic-MDETR [7]	ResNet-50	85.97	88.82	80.12	74.83	81.7	63.44	73.18	74.49
SimVG [5]	ViT-L	<b>90.61</b>	92.53	87.68	<b>85.36</b>	<b>89.61</b>	<b>79.74</b>	82.67	86.8
Grounding DINO[25]	Swin-L	90.56	<u>93.19</u>	<u>88.24</u>	82.75	88.95	75.92	<u>86.13</u>	<u>87.02</u>
AerialVG (Ours)	Swin-L	<u>90.58</u>	<b>93.23</b>	<b>88.56</b>	<u>82.83</u>	<u>89.02</u>	<u>76.03</u>	<b>86.52</b>	<b>88.04</b>

Table 3. **Ablation study.** Attn refers to hierarchical cross attention, Relation refers to relation aware grounding.

Method	AerialVG	
	Fine-Tuning	
	Top 1	Top 5
Grounding DINO (Baseline)	29.36	78.87
Grounding DINO + Attn	29.78	82.32
Grounding DINO + Relation	45.63	79.63
Grounding DINO + Attn +Relation	50.01	87.00

firms that the module helps disambiguate objects based on spatial and contextual relationships, rather than relying solely on visual appearance.



Figure 6. **Example of Qualitative Test.** Annotation: A blue car is parking on the right road with a white sedan above it. The model output score for this result is 0.70.

## 5.5. Qualitative Results

To better validate the generalization ability of our model, we conducted real-world experiments by capturing a set of aerial images using the DJI M30T drone. The images were taken at an altitude of 50 meters with a resolution of

4000×3000. The images are filled with various types of vehicles, posing a significant challenge to object localization. However, as shown in Figure 6, our model still successfully locates the objects accurately based on spatial relationship information, demonstrating its strong generalization capability. We will show more visualization results in the supplementary material.

## 6. Limitations and Future Work

The primary limitation of current visual grounding models, including our AerialVG, is their inability to effectively recognize unstructured background information, such as roads and other environmental elements. While these models excel at detecting foreground objects, they often struggle to incorporate contextual information from the background, which is crucial for tasks requiring a more holistic understanding of the scene. Promoting the spatial intelligence of perception models will be a key focus of our future work.

## 7. Conclusion

In this paper, we introduce AerialVG, a visual grounding task designed specifically for aerial perspectives. We construct the first real-world dataset tailored for this task, featuring high-resolution aerial imagery with densely populated scenes and complex spatial relationships. To address the challenges of fine-grained object differentiation and spatial reasoning, we propose an effective model, integrating Hierarchical Cross-Attention and a Relation-Aware Grounding module to enhance object localization accuracy. Extensive experiments validate the effectiveness of our approach, demonstrating state-of-the-art performance on the AerialVG dataset and competitive results on standard RefCOCO benchmarks. Our findings highlight the importance of spatial reasoning in aerial visual grounding and establish AerialVG as a challenging benchmark for future research. We hope that our dataset and the proposed method will serve as a solid foundation for advancing aerial view perception and autonomous vision-and-language applications.

## References

- [1] Cesar Cadena, Luca Carlone, Henry Carrillo, Yasir Latif, Davide Scaramuzza, José Neira, Ian Reid, and John J Leonard. Past, present, and future of simultaneous localization and mapping: Toward the robust-perception age. *IEEE Transactions on robotics*, 32(6):1309–1332, 2016. 3
- [2] Boyuan Chen, Zhuo Xu, Sean Kirmani, Brian Ichter, Danny Driess, Pete Florence, Dorsa Sadigh, Leonidas Guibas, and Fei Xia. Spatialvlm: Endowing vision-language models with spatial reasoning capabilities, 2024. 3
- [3] Qizhi Chen, Delin Qu, Yiwen Tang, Haoming Song, Yiting Zhang, Dong Wang, Bin Zhao, and Xuelong Li. Freegaussian: Guidance-free controllable 3d gaussian splats with flow derivatives. *arXiv preprint arXiv:2410.22070*, 2024. 3
- [4] An-Chieh Cheng, Hongxu Yin, Yang Fu, Qiushan Guo, Ruihan Yang, Jan Kautz, Xiaolong Wang, and Sifei Liu. Spatial-rgpt: Grounded spatial reasoning in vision-language models. *Advances in Neural Information Processing Systems*, 37:135062–135093, 2025. 3
- [5] Ming Dai, Lingfeng Yang, Yihao Xu, Zhenhua Feng, and Wankou Yang. Simvg: A simple framework for visual grounding with decoupled multi-modal fusion. *arXiv preprint arXiv:2409.17531*, 2024. 2, 7, 8
- [6] Wenliang Dai, Junnan Li, Dongxu Li, Anthony Meng Huat Tiong, Junqi Zhao, Weisheng Wang, Boyang Li, Pascale Fung, and Steven Hoi. Instructblip: Towards general-purpose vision-language models with instruction tuning, 2023. 3
- [7] Xiyang Dai, Yinpeng Chen, Jianwei Yang, Pengchuan Zhang, Lu Yuan, and Lei Zhang. Dynamic detr: End-to-end object detection with dynamic attention. In *Proceedings of the IEEE/CVF international conference on computer vision*, pages 2988–2997, 2021. 7, 8
- [8] Jiajun Deng, Zhengyuan Yang, Tianlang Chen, Wengang Zhou, and Houqiang Li. Transvg: End-to-end visual grounding with transformers, 2022. 2, 7, 8
- [9] Jacob Devlin, Ming-Wei Chang, Kenton Lee, and Kristina Toutanova. Bert: Pre-training of deep bidirectional transformers for language understanding, 2019. 5, 6
- [10] Henghui Ding, Chang Liu, Suchen Wang, and Xudong Jiang. Vision-language transformer and query generation for referring segmentation, 2021. 2
- [11] Hugh Durrant-Whyte and Tim Bailey. Simultaneous localization and mapping: part i. *IEEE robotics & automation magazine*, 13(2):99–110, 2006. 3
- [12] Huan Fu, Mingming Gong, Chaohui Wang, Kayhan Batmanghelich, and Dacheng Tao. Deep ordinal regression network for monocular depth estimation. In *Proceedings of the IEEE conference on computer vision and pattern recognition*, pages 2002–2011, 2018. 3
- [13] Akira Fukui, Dong Huk Park, Daylen Yang, Anna Rohrbach, Trevor Darrell, and Marcus Rohrbach. Multimodal compact bilinear pooling for visual question answering and visual grounding. *arXiv preprint arXiv:1606.01847*, 2016. 2
- [14] Yunpeng Gao, Chenhui Li, Zhongrui You, Junli Liu, Zhen Li, Pengan Chen, Qizhi Chen, Zhonghan Tang, Liansheng Wang, Penghui Yang, et al. Openfly: A versatile toolchain and large-scale benchmark for aerial vision-language navigation. *arXiv preprint arXiv:2502.18041*, 2025. 3
- [15] Theophile Gervet, Soumith Chintala, Dhruv Batra, Jitendra Malik, and Devendra Singh Chaplot. Navigating to objects in the real world. *Science Robotics*, 8(79):eadf6991, 2023. 3
- [16] Daniel Gordon, Aniruddha Kembhavi, Mohammad Rastegari, Joseph Redmon, Dieter Fox, and Ali Farhadi. Iqa: Visual question answering in interactive environments. In *Proceedings of the IEEE conference on computer vision and pattern recognition*, pages 4089–4098, 2018. 3
- [17] Zoey Guo, Yiwen Tang, Ray Zhang, Dong Wang, Zhigang Wang, Bin Zhao, and Xuelong Li. Viewreer: Grasp the multi-view knowledge for 3d visual grounding with gpt and prototype guidance, 2023. 2
- [18] Ziyu Guo, Renrui Zhang, Xiangyang Zhu, Yiwen Tang, Xianzheng Ma, Jiaming Han, Kexin Chen, Peng Gao, Xianzhi Li, Hongsheng Li, et al. Point-bind & point-llm: Aligning point cloud with multi-modality for 3d understanding, generation, and instruction following. *arXiv preprint arXiv:2309.00615*, 2023. 2
- [19] Marcel Hildebrandt, Hang Li, Rajat Koner, Volker Tresp, and Stephan Günnemann. Scene graph reasoning for visual question answering, 2020. 3
- [20] Yining Hong, Chunru Lin, Yilun Du, Zhenfang Chen, Joshua B. Tenenbaum, and Chuang Gan. 3d concept learning and reasoning from multi-view images, 2023. 3
- [21] Yining Hong, Haoyu Zhen, Peihao Chen, Shuhong Zheng, Yilun Du, Zhenfang Chen, and Chuang Gan. 3d-llm: Injecting the 3d world into large language models. *Advances in Neural Information Processing Systems*, 36:20482–20494, 2023. 3
- [22] Ke Li, Di Wang, Haojie Xu, Haodi Zhong, and Cong Wang. Language-guided progressive attention for visual grounding in remote sensing images. *IEEE Transactions on Geoscience and Remote Sensing*, 62:1–13, 2024. 2
- [23] Liunian Harold Li, Mark Yatskar, Da Yin, Cho-Jui Hsieh, and Kai-Wei Chang. Visualbert: A simple and performant baseline for vision and language, 2019. 2
- [24] Haotian Liu, Chunyuan Li, Qingyang Wu, and Yong Jae Lee. Visual instruction tuning, 2023. 3
- [25] Shilong Liu, Zhaoyang Zeng, Tianhe Ren, Feng Li, Hao Zhang, Jie Yang, Chunyuan Li, Jianwei Yang, Hang Su, Jun Zhu, et al. Grounding dino: Marrying dino with grounded pre-training for open-set object detection. *arXiv preprint arXiv:2303.05499*, 2023. 2, 5, 7, 8
- [26] Shubo Liu, Hongsheng Zhang, Yuankai Qi, Peng Wang, Yaning Zhang, and Qi Wu. Aerialvlm: Vision-and-language navigation for uavs, 2023. 3
- [27] Wei Liu, Dragomir Anguelov, Dumitru Erhan, Christian Szegedy, Scott Reed, Cheng-Yang Fu, and Alexander C Berg. Ssd: Single shot multibox detector. In *Computer Vision–ECCV 2016: 14th European Conference, Amsterdam, The Netherlands, October 11–14, 2016, Proceedings, Part I* 14, pages 21–37. Springer, 2016. 2
- [28] Yongfei Liu, Bo Wan, Xiaodan Zhu, and Xuming He. Learning cross-modal context graph for visual grounding. In *Proceedings of the AAAI conference on artificial intelligence*, pages 11645–11652, 2020. 2

- [29] Ze Liu, Yutong Lin, Yue Cao, Han Hu, Yixuan Wei, Zheng Zhang, Stephen Lin, and Baining Guo. Swin transformer: Hierarchical vision transformer using shifted windows, 2021. [5](#), [6](#)
- [30] Varun K. Nagaraja, Vlad I. Morariu, and Larry S. Davis. Modeling context between objects for referring expression understanding, 2016. [7](#)
- [31] OpenAI, Josh Achiam, Steven Adler, Sandhini Agarwal, Lama Ahmad, Ilge Akkaya, Florencia Leoni Aleman, Diogo Almeida, Janko Altenschmidt, Sam Altman, Shyamal Anadkat, Red Avila, Igor Babuschkin, Suchir Balaji, Valerie Balcom, Paul Baltescu, Haiming Bao, Mohammad Bavarian, Jeff Belgum, Irwan Bello, Jake Berdine, Gabriel Bernadett-Shapiro, Christopher Berner, Lenny Bogdonoff, Oleg Boiko, Madelaine Boyd, Anna-Luisa Brakman, Greg Brockman, Tim Brooks, Miles Brundage, Kevin Button, Trevor Cai, Rosie Campbell, Andrew Cann, Brittany Carey, Chelsea Carlson, Rory Carmichael, Brooke Chan, Che Chang, Fotis Chantzis, Derek Chen, Sully Chen, Ruby Chen, Jason Chen, Mark Chen, Ben Chess, Chester Cho, Casey Chu, Hyung Won Chung, Dave Cummings, Jeremiah Currier, Yunxing Dai, Cory Decareaux, Thomas Degry, Noah Deutsch, Damien Deville, Arka Dhar, David Dohan, Steve Dowling, Sheila Dunning, Adrien Ecoffet, Atty Eleti, Tyna Eloundou, David Farhi, Liam Fedus, Niko Felix, Simón Posada Fishman, Juston Forte, Isabella Fulford, Leo Gao, Elie Georges, Christian Gibson, Vik Goel, Tarun Gogneni, Gabriel Goh, Rapha Gontijo-Lopes, Jonathan Gordon, Morgan Grafstein, Scott Gray, Ryan Greene, Joshua Gross, Shixiang Shane Gu, Yufei Guo, Chris Hallacy, Jesse Han, Jeff Harris, Yuchen He, Mike Heaton, Johannes Heidecke, Chris Hesse, Alan Hickey, Wade Hickey, Peter Hoeschele, Brandon Houghton, Kenny Hsu, Shengli Hu, Xin Hu, Joost Huizinga, Shantanu Jain, Shawn Jain, Joanne Jang, Angela Jiang, Roger Jiang, Haozhun Jin, Denny Jin, Shino Jomoto, Billie Jonn, Heewoo Jun, Tomer Kaftan, Łukasz Kaiser, Ali Kamali, Ingmar Kanitscheider, Nitish Shirish Keskar, Tabarak Khan, Logan Kilpatrick, Jong Wook Kim, Christina Kim, Yongjik Kim, Jan Hendrik Kirchner, Jamie Kiros, Matt Knight, Daniel Kokotajlo, Łukasz Kondraciuk, Andrew Kondrich, Aris Konstantinidis, Kyle Kosic, Gretchen Krueger, Vishal Kuo, Michael Lampe, Ikai Lan, Teddy Lee, Jan Leike, Jade Leung, Daniel Levy, Chak Ming Li, Rachel Lim, Molly Lin, Stephanie Lin, Mateusz Litwin, Theresa Lopez, Ryan Lowe, Patricia Lue, Anna Makanju, Kim Malfacini, Sam Manning, Todor Markov, Yaniv Markovski, Bianca Martin, Katie Mayer, Andrew Mayne, Bob McGrew, Scott Mayer McKinney, Christine McLeavey, Paul McMillan, Jake McNeil, David Medina, Aalok Mehta, Jacob Menick, Luke Metz, Andrey Mishchenko, Pamela Mishkin, Vinnie Monaco, Evan Morikawa, Daniel Mossing, Tong Mu, Mira Murati, Oleg Murk, David Mély, Ashvin Nair, Rei-ichi Nakano, Rajeev Nayak, Arvind Neelakantan, Richard Ngo, Hyeonwoo Noh, Long Ouyang, Cullen O’Keefe, Jakub Pachocki, Alex Paino, Joe Palermo, Ashley Pantuliano, Giambattista Parascandolo, Joel Parish, Emy Parparita, Alex Passos, Mikhail Pavlov, Andrew Peng, Adam Perelman, Filipe de Avila Belbute Peres, Michael Petrov, Henrique Ponde de Oliveira Pinto, Michael Pokorny, Michelle Pokrass, Vitchyr H. Pong, Tolly Powell, Alethea Power, Boris Power, Elizabeth Proehl, Raul Puri, Alec Radford, Jack Rae, Aditya Ramesh, Cameron Raymond, Francis Real, Kendra Rimbach, Carl Ross, Bob Rotstet, Henri Roussez, Nick Ryder, Mario Saltarelli, Ted Sanders, Shibani Santurkar, Girish Sastry, Heather Schmidt, David Schnurr, John Schulman, Daniel Selsam, Kyla Sheppard, Toki Sherbakov, Jessica Shieh, Sarah Shoker, Pranav Shyam, Szymon Sidor, Eric Sigler, Maddie Simens, Jordan Sitkin, Katarina Slama, Ian Sohl, Benjamin Sokolowsky, Yang Song, Natalie Staudacher, Felipe Petroski Such, Natalie Summers, Ilya Sutskever, Jie Tang, Nikolas Tezak, Madeleine B. Thompson, Phil Tillett, Amin Toootoonchian, Elizabeth Tseng, Preston Tuggle, Nick Turley, Jerry Tworek, Juan Felipe Cerón Uribe, Andrea Valalone, Arun Vijayvergiya, Chelsea Voss, Carroll Wainwright, Justin Jay Wang, Alvin Wang, Ben Wang, Jonathan Ward, Jason Wei, CJ Weinmann, Akila Welihinda, Peter Welinder, Jiayi Weng, Lilian Weng, Matt Wiethoff, Dave Willner, Clemens Winter, Samuel Wolrich, Hannah Wong, Lauren Workman, Sherwin Wu, Jeff Wu, Michael Wu, Kai Xiao, Tao Xu, Sarah Yoo, Kevin Yu, Qiming Yuan, Wojciech Zaremba, Rowan Zellers, Chong Zhang, Marvin Zhang, Shengjia Zhao, Tianhao Zheng, Juntang Zhuang, William Zhuk, and Barret Zoph. Gpt-4 technical report, 2024. [3](#)
- [32] Delin Qu, Qizhi Chen, Pingui Zhang, Xianqiang Gao, Bin Zhao, Dong Wang, and Xuelong Li. Livescene: Language embedding interactive radiance fields for physical scene rendering and control. *arXiv preprint arXiv:2406.16038*, 2024. [3](#)
- [33] Delin Qu, Haoming Song, Qizhi Chen, Yuanqi Yao, Xinyi Ye, Yan Ding, Zhigang Wang, JiaYuan Gu, Bin Zhao, Dong Wang, and Xuelong Li. Spatialvlva: Exploring spatial representations for visual-language-action model, 2025. [3](#)
- [34] J Redmon. You only look once: Unified, real-time object detection. In *Proceedings of the IEEE conference on computer vision and pattern recognition*, 2016. [2](#)
- [35] Shaoqing Ren, Kaiming He, Ross Girshick, and Jian Sun. Faster r-cnn: Towards real-time object detection with region proposal networks. *IEEE transactions on pattern analysis and machine intelligence*, 39(6):1137–1149, 2016. [2](#)
- [36] Yiwen Tang, Hongbo Chen, Liyue Qian, Songhan Ge, Mingbo Zhang, and Rui Zheng. Detection of spine curve and vertebral level on ultrasound images using detr. In *2022 IEEE international ultrasonics symposium (IUS)*, pages 1–4. IEEE, 2022. [2](#)
- [37] Yiwen Tang, Ray Zhang, Zoey Guo, Xianzheng Ma, Bin Zhao, Zhigang Wang, Dong Wang, and Xuelong Li. Point-peft: Parameter-efficient fine-tuning for 3d pre-trained models. In *Proceedings of the AAAI Conference on Artificial Intelligence*, pages 5171–5179, 2024.
- [38] Yiwen Tang, Ray Zhang, Jiaming Liu, Zoey Guo, Bin Zhao, Zhigang Wang, Peng Gao, Hongsheng Li, Dong Wang, and Xuelong Li. Any2point: Empowering any-modality large models for efficient 3d understanding. In *European Conference on Computer Vision*, pages 456–473. Springer, 2024. [2](#)

- [39] Yiwen Tang, Zoey Guo, Zuhao Wang, Ray Zhang, Qizhi Chen, Junli Liu, Delin Qu, Zhigang Wang, Dong Wang, Xuelong Li, and Bin Zhao. Exploring the potential of encoder-free architectures in 3d lmms, 2025. 3
- [40] Johanna Wald, Helisa Dhamo, Nassir Navab, and Federico Tombari. Learning 3d semantic scene graphs from 3d indoor reconstructions. *2020 IEEE/CVF Conference on Computer Vision and Pattern Recognition (CVPR)*, 2020. 3
- [41] Liwei Wang, Yin Li, Jing Huang, and Svetlana Lazebnik. Learning two-branch neural networks for image-text matching tasks. *IEEE Transactions on Pattern Analysis and Machine Intelligence*, 41(2):394–407, 2018. 2
- [42] Bin Xiao, Haiping Wu, Weijian Xu, Xiyang Dai, Houdong Hu, Yumao Lu, Michael Zeng, Ce Liu, and Lu Yuan. Florence-2: Advancing a unified representation for a variety of vision tasks, 2023. 2
- [43] Haiyang Xu, Qinghao Ye, Ming Yan, Yaya Shi, Jiabo Ye, Yuanhong Xu, Chenliang Li, Bin Bi, Qi Qian, Wei Wang, Guohai Xu, Ji Zhang, Songfang Huang, Fei Huang, and Jingen Zhou. mplug-2: A modularized multi-modal foundation model across text, image and video, 2023. 2
- [44] Runsen Xu, Xiaolong Wang, Tai Wang, Yilun Chen, Jiangmiao Pang, and Dahua Lin. Pointllm: Empowering large language models to understand point clouds, 2024. 3
- [45] Bin Yan, Yi Jiang, Jannan Wu, Dong Wang, Ping Luo, Ze-huan Yuan, and Huchuan Lu. Universal instance perception as object discovery and retrieval. In *Proceedings of the IEEE/CVF Conference on Computer Vision and Pattern Recognition*, pages 15325–15336, 2023. 2
- [46] Licheng Yu, Patrick Poirson, Shan Yang, Alexander C. Berg, and Tamara L. Berg. Modeling context in referring expressions, 2016. 7
- [47] Zhihao Yuan, Jinke Ren, Chun-Mei Feng, Hengshuang Zhao, Shuguang Cui, and Zhen Li. Visual programming for zero-shot open-vocabulary 3d visual grounding, 2024. 2
- [48] Yan Zeng, Xinsong Zhang, Hang Li, Jiawei Wang, Jipeng Zhang, and Wangchunshu Zhou. X<sup>2</sup>-vlm: All-in-one pre-trained model for vision-language tasks, 2023. 2
- [49] Haotian\* Zhang, Pengchuan\* Zhang, Xiaowei Hu, Yen-Chun Chen, Liunian Harold Li, Xiyang Dai, Lijuan Wang, Lu Yuan, Jenq-Neng Hwang, and Jianfeng Gao. Glipv2: Unifying localization and vision-language understanding. *arXiv preprint arXiv:2206.05836*, 2022. 6
- [50] Renrui Zhang, Han Qiu, Tai Wang, Ziyu Guo, Ziteng Cui, Yu Qiao, Hongsheng Li, and Peng Gao. Monodetr: Depth-guided transformer for monocular 3d object detection. In *Proceedings of the IEEE/CVF International Conference on Computer Vision*, pages 9155–9166, 2023. 2
- [51] Ruijie Zheng, Yongyuan Liang, Shuaiyi Huang, Jianfeng Gao, Hal Daumé III, Andrey Kolobov, Furong Huang, and Jianwei Yang. Tracevla: Visual trace prompting enhances spatial-temporal awareness for generalist robotic policies, 2024. 3
- [52] Fengda Zhu, Yi Zhu, Xiaojun Chang, and Xiaodan Liang. Vision-language navigation with self-supervised auxiliary reasoning tasks. In *Proceedings of the IEEE/CVF conference on computer vision and pattern recognition*, pages 10012–10022, 2020. 2
- [53] Pengfei Zhu, Longyin Wen, Dawei Du, Xiao Bian, Heng Fan, Qinghua Hu, and Haibin Ling. Detection and tracking meet drones challenge. *IEEE Transactions on Pattern Analysis and Machine Intelligence*, 44(11):7380–7399, 2021. 4